 DLR	MAPP ATBD	Chlorophyll map
--	----------------------------	------------------------

Title: **Chlorophyll Map**


Doc. no: MAPP-ATBD-CMAP

Issue: 1

Revision: 0

Date: 03/12/99

Author: K. P. Günther, S. Maier
DLR – German Aerospace Center
DFD - German Remote Sensing Data Center
Climate and Atmospheric Products
D - 82 230 - Wessling
Germany

	Chlorophyll map ATBD	Doc. ID : MAPP-ATBD-CMAP Name : Chlorophyll Map Issue : 1 Rev.: 0 Date : 03/12/99 Page : ii
---	---	--

internal Distribution

Name

Quantity

external Distribution

Name

Quantity

Change Record

Issue

Revision

Date

Description

Change pages


	Chlorophyll map ATBD	Doc. ID : MAPP-ATBD-CMAP Name : Chlorophyll Map Issue : 1 Rev.: 0 Date : 03/12/99 Page : iii
---	---	---

Table of Contents

1. INTRODUCTION.....	1
1.1 ALGORITHM IDENTIFICATION.....	1
2. ALGORITHM OVERVIEW.....	1
3. ALGORITHM DESCRIPTION.....	2
3.1 THEORETICAL DESCRIPTION.....	2
3.1.1 <i>Mathematical Description of the Algorithm</i>	2
3.1.1.1 Modeling the RRVI and the RGVI for MOS specification	3
3.1.1.2 Simulation of leaf reflectance	3
3.1.1.3 Simulation of canopy reflectance.....	4
3.1.2 <i>Results</i>	6
3.1.2.1 Modeling RRVI and RGVI for leaves.....	6
3.1.2.2 Influence of scan angle (observation geometry)	7
3.1.2.3 Influence of sun zenith angle.....	8
3.1.2.4 Influence of canopy structure.....	10
3.1.2.5 Influence of leaf area index (LAI) and leaf angle distribution function (LADF)	11
3.1.2.6 RRVI depending on leaf chlorophyll content.....	13
3.1.2.7 RGVI depending on leaf chlorophyll content	15
3.1.2.8 Summary	18
3.2 PRACTICAL CONSIDERATIONS.....	20
3.2.1 <i>Numerical computation considerations</i>	21
3.2.2 <i>Calibration and Validation</i>	21
3.2.3 <i>Exception Handling</i>	21
3.2.4 <i>Output Products</i>	21
4. ERROR BUDGET ESTIMATES	21
5. REFERENCES.....	21
6. MAPP DATA PRODUCT SUMMARY SHEET	22
7. ACKNOWLEDGEMENT	23



MERIS

Doc : MAPP-ATBD-CMAP
Name : Chlorophyll Map
Issue : 1 **Rev** : 0
Date : 08/06/99
Page : 1

1. INTRODUCTION

1.1 Algorithm Identification

The experimental chlorophyll map product will be based on full resolution MERIS level-2 BOA reflectances delivered as standard products from ESA. Only two spectral channels will be used in addition with MERIS flags as e.g. land and water identification, cloud detection etc.

The chlorophyll map will be delivered for every orbit path and stored temporarily. A subsequent sampling procedure (in time) will be applied in order to minimise data gaps due to clouds.

Spatial resolution: 300 m

Temporal resolution: every orbit and a composite over 9 days

2. ALGORITHM OVERVIEW

The reflectance spectra of leaves in the course from greening to autumnal senescence show a dramatic variation due to the in- and decrease of chlorophyll pigments (Chl a and Chl b). The signature analysis of reflectance spectra measured during autumnal senescence indicates that maximal standard deviation is found near 550 to 560 nm and near 700 to 710 nm (Gitelson and Merzylak 1994). The revealed spectral features can serve as sensitive indicators of chlorophyll content of leaves. Several indicators as e.g. the reflectance ratios $R750/R705$, $R750/R555$ and the vegetation index $(R750 - R705) / (R750 + R705)$ were found to be linearly proportional to the chlorophyll a content showing correlation coefficients of more than 0.96. Gitelson and Merzylak (1994) and Gitelson and Merzylak (1996) found that linearity is valid in the dynamic of the chlorophyll content from about $0.5 \mu\text{g}/\text{cm}^2$ up to about $25 \mu\text{g}/\text{cm}^2$ (for leaves of chestnut, *Aesculus hippocastanum* L., and maple, *Acer platanoides* L.). The estimation error is less than about $1.5 \mu\text{g}/\text{cm}^2$.

This linear behavior in contrast to the well known non – linear behavior of the NDVI (defined as: $(R750 - R675) / (R675 + R750)$) with chlorophyll content can be explained as follows. In the main red absorption bands of chlorophyll a saturation occurs for pigment contents of more than $10 \mu\text{g}/\text{cm}^2$. Healthy, green leaves show chlorophyll contents up to $60 \mu\text{g}/\text{cm}^2$. In order to deduce chlorophyll content from reflectance spectra the "chlorophyll sensitive" wavelength should not be situated in the maximum of the absorption band (e.g. at 675 nm) but as close as possible to the absorption band (e.g. in the red range from 700 to 710 nm).

The findings of Gitelson and Merzylak (1994, 1997) are summarized in table 1. It is shown that for the determination of chlorophyll a and chlorophyll a+b a high linear correlation exists for all vegetation indices.



Species		a	b	r ²	Est. error
Maple / chestnut (chl \bar{a}) *	R750 / R705	- 11.75	15.0	0.98	1.52
Maple / chestnut (chl \bar{a}) *	R750 / R555	-7.3	8.59	0.974	1.77
Maple / chestnut (chl \bar{a}) *	(R750-R705)/(R750+R705)	-0.945	58.91	0.969	1.94
Different leaves (chl \bar{a} + \bar{b}) **	R750 / R550	-12.7	13.7	0.90	5.3
Different leaves (chl \bar{a} + \bar{b}) **	R750 / R700	-12.5	13.29	0.93	4.5

Table 1: Results of Gitelson and Merzylak (1994, *) and Gitelson and Merzylak (1997, **) for the linear correlation of different vegetation indices with the chlorophyll content of leaves.

3. ALGORITHM DESCRIPTION

As mentioned before, a simple vegetation index can be applied for deriving the chlorophyll content of leaves. In order to use a vegetation index based on MERIS data for deriving chlorophyll maps of canopies, it is necessary to model the influence of canopy structure, illumination and observation geometry, soil background and leaf parameters as e.g. leaf pigment contents. This task will be described in detail in the next chapter.

For all modelling purposes, the leaf parameters given by Gitelson and Merzylak (1994) will be checked for suitability to describe canopy parameter.

3.1 Theoretical Description

3.1.1 Mathematical Description of the Algorithm

The "Red-Red-vegetation index" (RRVI) for leaves according to Gitelson and Merzylak (1994) is defined by the following equation:

$$RRVI = \rho_2 / \rho_1$$

with ρ_1 and ρ_2 as diffuse reflectances at 705 nm and 750 nm, respectively, measured with a high-resolution radiometer (spectral resolution of 1nm) attached to an integrating sphere. The diffuse reflectances are calculated with barium sulfate as reference. The reflectance measurements were performed with black velvet behind the leaves in order to absorb transmitted light. Interpreting this procedure in term of canopy architecture it is equivalent to a canopy with a leaf area index (LAI) of 1 over a black soil.

In order to derive from MERIS data a MERIS_RRVI the following equation will hold:

$$MERIS_RRVI = \rho_2 / \rho_1$$

With ρ_2 as the BOA-reflectance at 753,75nm (corresponding to MERIS channel 10) and ρ_1 as the BOA-reflectance at 705 nm (corresponding to MERIS channel 9).

In addition, Gitelson and Merzylak (1994) developed the "Red-Green-Vegetation -Index" (RGVI) which is defined as follows:

$$RGVI = \rho_2 / \rho_1$$



MERIS

Doc : MAPP-ATBD-CMAP
Name : Chlorophyll Map
Issue : 1 **Rev** : 0
Date : 08/06/99
Page : 3

with ρ_1 and ρ_2 as diffuse reflectances at 555 nm and 750 nm, respectively. The reflectances are determined as described before. Analogue to the RRVI, the MERIS_RGVI is defined as:

$$\text{MERIS_RGVI} = \rho_2 / \rho_1$$

With ρ_2 as the BOA-reflectance at 753,75nm (corresponding to MERIS channel 10) and ρ_1 as the BOA-reflectance at 560 nm (corresponding to MERIS channel 5).

The interest of the following section is to show that the MERIS_RRVI or the MERIS_RGVI is a good, reliable parameter for determining canopy chlorophyll content. A coupled leaf-canopy model will be used for analyzing the influence of canopy architecture, soil conditions (different leaf parameters, different canopy structures) and the observation geometries occurring during a year for MERIS passing the M1 grid. The M1 grid is the area where most MAPP products should be valid.

3.1.1.1 Modeling the RRVI and the RGVI for MOS specification

The leaf parameter presented by Gitelson and Merzylak (1994) will be checked for their usefulness for describing canopy conditions as e.g the chlorophyll content. Due to the fact that MERIS data are not yet available, a pre-launch test will be performed based on MOS data. Therefore, all model calculation are first performed using MOS specification (spectral characteristics, swath width, orbit characteristics etc.)

The new parameter MOS_RRVI and MOS_RGVI are introduced according to:

$$\text{MOS_RRVI} = \rho_2 / \rho_1$$

With ρ_2 as the BOA-reflectance at 750 nm (corresponding to MOS channel 9) and ρ_1 as the BOA-reflectance at 685 nm (corresponding to MOS channel 8).

$$\text{MOS_RGVI} = \rho_2 / \rho_1$$

With ρ_2 as the BOA-reflectance at 750 nm (corresponding to MOS channel 9) and ρ_1 as the BOA-reflectance at 570 nm (corresponding to MOS channel 5).

3.1.1.2 Simulation of leaf reflectance

Leaf reflectance and leaf transmittance are modeled using the SLOP model (Stochastic model for Leaf Optical Properties) of Maier (1996). SLOP is based on the stochastic optical leaf model of Tucker and Garratt (1977) and the extended version developed by Luedeker and Guenther (1990). The extended model was revised, taking into account additional leaf components as e.g. the proteins, the lignins and in the future UV - protecting pigments located in the epidermal layer.

The extended model takes into account different mechanisms like absorption, reflection and scattering at the chloroplasts and the leaf cells as well as a new radiation state for the backscattered light from the spongy parenchyma. In addition the transition probabilities were modified.

With the revised Stochastic model for Leaf Optical Properties SLOP the reflection, transmission and absorption of light by leaves can be calculated in the spectral region from 400 nm up to 2.5 μm . The model treats the radiative transfer of diffuse light as transitions of light with weighted probabilities according to the theory of homogeneous Markov chains with a finite number of states. The leaves are divided in several compartments analogue to the well known leaf structure. A new radiation state is introduced for regarding the absorption in the epidermal layer, while in the palisade and spongy parenchyma the light is absorbed and scattered depending on their pigment concentration and the scattering efficiencies. The transition probabilities are determined by the optical properties of the leaf and the geometric leaf structure. The main parameters of the model are the concentrations and specific absorption coefficients of chlorophyll a and b , the accessory pigments (beta-carotene, lutein, violaxanthin, anthocyanin), proteins, cellulose, lignin and water. The specific absorption coefficients measured in alcoholic solutions are taken from the literature. The scattering coefficients and the

thickness of the palisade and spongy parenchyma are also input parameters as well as the number of chloroplasts. The upper and lower epidermis is regarded as scattering element. Therefore the a priori knowledge of the reflectance spectrum is not necessary, in contrast to the commonly used semi-empirical models.

The model is now fully operational. The reflectance and transmittance spectra when changing the leaf parameter can be visualized in near real time. The algorithm is implemented as a macro function in an EXCEL sheet.

A typical result for the reflectance and transmittance of a green leaf is presented in figure 1. The chlorophyll a and b concentration is about $32 \mu\text{g} / \text{cm}^2$, the water equivalent thickness is 0.008 cm.

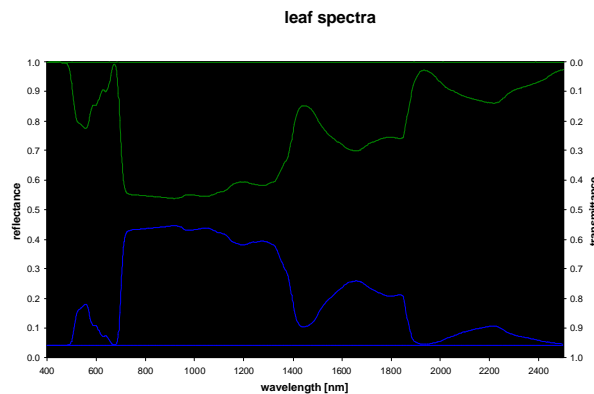


Figure 1: Reflectance (blue) and transmittance (green) of a green leaf, calculated by the SLOP model of Maier et al. (1999). The constant reflection is attributed to Fresnel reflectance at the leaf surface.

The reflectance and transmittance spectrum shown in figure 1 is used for modelling the canopy reflectance of green vegetation.

3.1.1.3 Simulation of canopy reflectance

In recent years many canopy radiative transfer models have been developed as e.g. the fast 2-stream model SAIL (Verhoef, 1984; Braswell et al., 1996), or on the other hand the highly complex 3-dimensional photon transport model 3-D DISORD (Myneni and Asrar, 1993), which is considered the most accurate but computationally expensive. The SAIL model is selected for modelling canopy reflectance since it produces nadir and off-nadir reflectance values with reasonable accuracy (e.g., Major et al., 1992; Huemmrich and Goward, 1997).

The SAIL model produces top-of-canopy reflectance values and needs the following input parameters:

- leaf area index (LAI)
- leaf angle distributions (LADF)
- leaf hemispherical reflectance $\rho_{\text{leaf}}(\lambda)$
- leaf transmittance $\tau_{\text{leaf}}(\lambda)$
- soil reflectance $\rho_{\text{soil}}(\lambda)$

- sun and view zenith and azimuth angles (Θ_{sun} , Φ_{sun} , Θ_{view} , Φ_{view}) and
- hot-spot parameter for each vegetation component ($\text{SIZE}_{\text{leaf}}$)

The hemispherical leaf reflectance and transmittance spectra will be calculated by the SLOP model which has the following inputs:

- pigment concentration (e.g. chlorophyll and carotenoids)
- water content
- leaf thickness including thickness of the palisade and spongy parenchyma and
- isotropic scattering coefficient in the leaf

In the past Jacquemoud et. al. (1995) inverted a coupled leaf – canopy transfer model (the PROSPECT – SAIL model) for extracting biophysical parameter of sugar beet from remote sensing data (AVIRIS and TM). Based on this work, we developed our coupled SLOP – SAIL model supported by S. Jacquemoud.

As an example, a variation of the observation zenith angle from -80° to 80° results in a variation of the reflectance at 805 nm from about 0.42 to about 0.80 while the other parameters (leaf reflectance and transmittance, soil reflectance, leaf angle distribution function, leaf area index, sun zenith angle and visibility) are fixed. The detailed results for different parameters of the canopy structure ("hot spot parameter") are shown in figure 2 which can be used for comparison with the results of Jacquemoud et al (1995) presented in figure 2 of his paper.

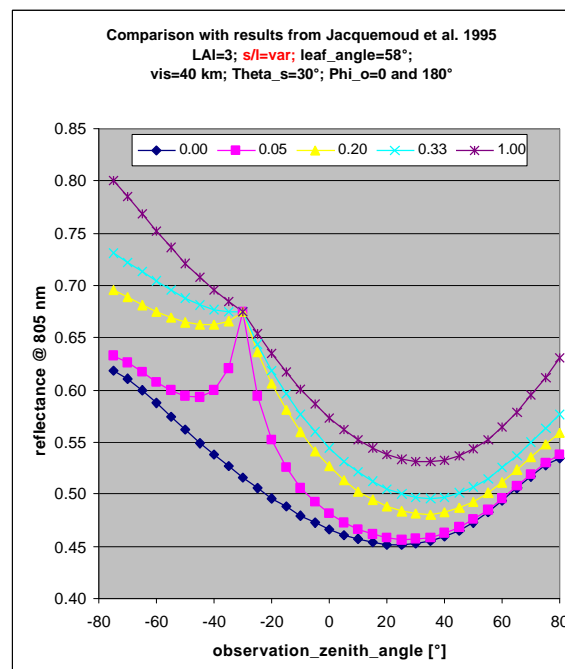


Figure 2: Variation of the canopy reflectance at 805 nm simulated by the coupled SLOP – SAIL model as a function of the observation zenith angle and the canopy structure parameter s/l ("hot-spot parameter"). s/l varies from 0 (no hot spot) to 1.

The reflectance functions of the coupled leaf-canopy model were used for calculating the signals for MERIS. The simulation assumes Gaussian like transmission function for the MERIS channels.



3.1.2 Results

3.1.2.1 Modeling RRVI, RGVI, Green_AVHRR and AVHRR_NDVI for leaves

In order to test the coupled leaf –canopy model, the statement of Gitelson and Merzylak (1994) was tested that the RGVI ($R750 / R570$ for MOS specification) is linearly correlated with the chlorophyll content of leaves. As shown in figure 3, the "Red-Green-Vegetation –Index" RGVI (as measured by the MOS sensor) increases linearly with the total chlorophyll $a + b$ content. The chlorophyll content is ranging from 0 up to $62 \mu\text{g}/\text{cm}^2$. The algorithm for chlorophyll determination has the form $[\text{chl } a + b] = a + b * \text{RGVI}$. The regression analysis gives for the interception a value of $-8.023 [\mu\text{g} / \text{cm}^2]$ and for the slope a value of 9.58. The correlation coefficient r^2 is 0.9985. For comparison Gitelson and Merzylak (1994) found for the interception a value of $-7.3 [\mu\text{g} / \text{cm}^2]$ and for the slope a value of 8.59. It should be remarked that for the data shown in figure 3 the total chlorophyll content is given assuming a constant chlorophyll a to b ratio of three. Gitelson and Merzylak (1994) found a linear regression with the chlorophyll a content.

The "Red-Red-Vegetation –Index" presented here as the reflectance ratio $R750/R685$ is linear from 0 up to about $30 \mu\text{g}/\text{cm}^2$ total chlorophyll $a + b$ content. For higher chlorophyll contents the typical saturation is found as it is well known for the AVHRR_NDVI. Assuming the same algorithm as shown above for the chlorophyll determination the interception is $-4.23 [\mu\text{g} / \text{cm}^2]$ and the slope is 3.81. Gitelson and Merzylak (1994) using the reflectance ratio $R750/R705$ found different values for the interception (-11.75) and the slope (15.0). This difference in the findings for the interception and the slope demonstrates the sensitivity of the red-red reflectance ratio on the wavelength position near to the maximum of chlorophyll absorption.

In addition, the Green_NDVI defined as

$$\text{Green_NDVI} = (R750 - R685) / (R750 + R685)$$

was calculated in dependence of the total leaf chlorophyll content (Fig. 3) together with the conventional AVHRR_NDVI. Both parameter show the typical saturation at high chlorophyll content whereby the saturation of the Green_NDVI occurs beyond $25 \mu\text{g} / \text{cm}^2$ while the saturation of the AVHRR_NDVI occurs beyond $10 - 15 \mu\text{g} / \text{cm}^2$. The linear relationship for determining the total chlorophyll content of leaves from the Green_NDVI (according to the assumption of the same algorithm as shown above) gives an interception of $-4.4 [\mu\text{g} / \text{cm}^2]$ and a slope of 57.14. The correlation coefficient r^2 is 0.9711. Gitelson and Merzylak (1994) found an interception of $-0.945 [\mu\text{g} / \text{cm}^2]$ and a slope of 58.91 for the determination of the chlorophyll a content.

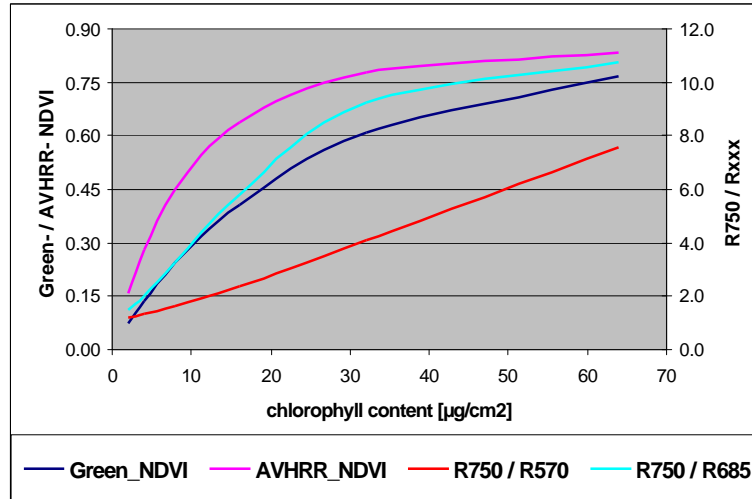


Fig. 3: Modeled Green-NDVI and AVHRR-NDVI (left y-axis) as well as reflectance ratios R750/R570; R750/R685 (right y-axis) of single leaves as a function of chlorophyll content.

3.1.2.2 Influence of scan angle (observation geometry)

In the following paragraphs a systematic investigation is presented analyzing the influence of different parameters as e.g. the observation or scan angle on the reflectance ratios given by Gitelson and Merzylak (1994). A typical observation and illumination geometry for the MOS sensor on board of the IRS-1C satellite was selected for the 5th July (day of the year: 217) over Sweden (within the M1 grid, defined as the operating area for the MAPP project). The sun zenith angle is about 46°. For the canopy architecture a leaf area index (LAI) of 3 is assumed as well as a random leaf angle distribution. Dark soil is taken in combination with light green leaves of 2 $\mu\text{g}/\text{cm}^2$ total chlorophyll. The coupled leaf-canopy model shows that for the MOS observation geometry ($\pm 8^\circ$) a variation of less than 0.15% for the reflectance ratios is expected. For RRVI a mean value of 1.93 ± 0.0026 is found while for RGVI a mean value of 1.41 ± 0.002 is calculated (figure 4).

For other chlorophyll contents, for several days of the year and for different canopy structures it is found that the variation of the reflectance ratio RGVI with scan angle is less than 0.8% and that the variation of the reflectance ratio RRVI with scan angle is less than 1.5%.

Model calculations taking into account the observation geometry of MERIS will be performed later.

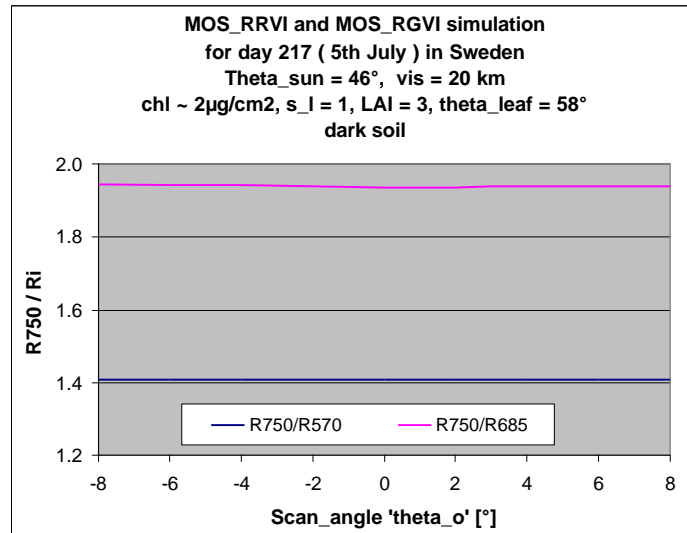


Figure 4: Modeled reflectance ratios RRVI and RGVI as a function of the scan angle (typical for the MOS sensor). The illumination and observation geometry for day 217 of the year (5th July) in Sweden was selected (sun zenith angle = 46°). LAI of the canopy was 3 with random leaf angle distribution, dark soil and ~2 µg/cm² total chlorophyll content.

3.1.2.3 Influence of sun zenith angle

For a fixed observation geometry (scan angle = 8°) and a well defined canopy in terms of leaf angle distribution function (58°), LAI (3), hot spot parameter (s_l=1), soil conditions and chlorophyll content of the leaves the influence of varying sun zenith angles on the reflectance ratios RRVI and RGVI is calculated using the coupled leaf-canopy model. As can be seen in figure 5, for a random of leaf angle distribution the RRVI increases by about 60% from the value where the sun is in the nadir direction (RRVI ~ 10,2) to about 60° sun zenith angle (RRVI ~16,1). All other parameters are held constant.

The RGVI in contrast increases by about 10 % from the sun in nadir position to sun zenith angles of about 60°. Assuming a mean RGVI which corresponds to a sun zenith angle of about 35°, only 5% variation must be considered.

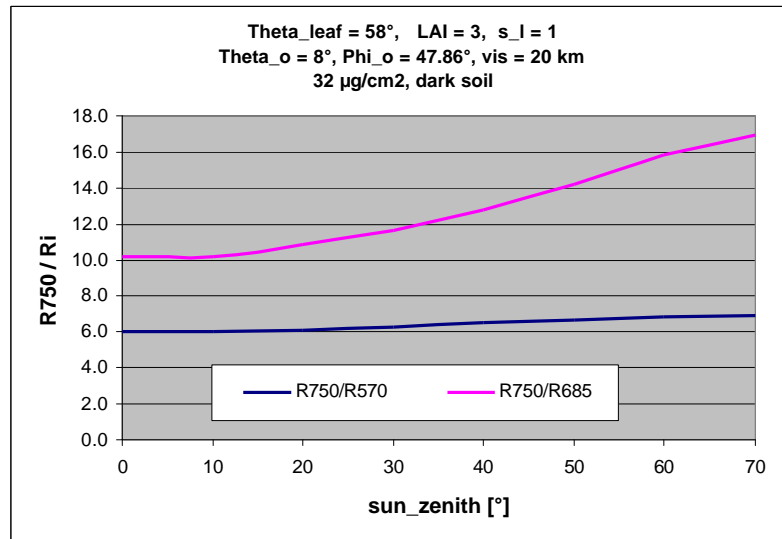


Figure 5: Modeled reflectance ratios RRVI and RGVI as a function of the sun zenith angle for dark green leaves ($32 \mu\text{g}/\text{cm}^2$) in a canopy with random leaf angle distribution function, LAI of 3. Dark soil is assumed as background.

Changing the leaf angle distribution function systematically from a planophile architecture (15°) to an erectophile architecture (75°) reveals that the influence of the sun zenith angle on both VI's increases when the leaf angle distribution function goes from planophile to erectophile.

As can be seen from figure 5 the RGVI has a weak increase with increasing sun zenith angle for a random oriented plant canopy. This statement also holds for other canopy architectures (table 2). Looking for the specific situation within the M1 grid from March till October (when remote sensing of land surfaces becomes meaningful), one can state, that the sun zenith angle will vary from about 60° (in March in northern Sweden) to about 20° (in summer in northern Africa). Thus, for a first approximation, it can be assumed that the RGVI is independent on the sun zenith angle for observations within the M1 grid.

Table 2 gives an overview of the range of both VI's (RRVI and RGVI), the mean value and the standard deviation in % of the mean value when the leaf angle distribution function is changed from a planophile to an erectophile canopy structure.

	15°	58°	75°
	Planophile	Random	Erectophile
min RRVI - max RRVI	13,6 – 15,9	10,2 – 16,4	4,7 – 18,2
<RRVI>	14,6	13,3	9,8
Std	5,5%	20,6%	53%
min RGVI - max RGVI	6,2 – 6,8	6,1 – 6,8	4,6 – 6,9
<RGVI>	6,5	6,5	5,9
std	3,3%	5,2	15,4%

Table 2: Variation of the RRVI and the RGVI for different canopy architecture (planophile, random and erectophile) with changing sun zenith angles ($0^\circ - 70^\circ$).

3.1.2.4 Hot spot parameter

The hot parameter s_l characterizes the amount of directly reflected sun light when the observer looks in the direction of the sun. The hot spot parameter s_l is defined as the ratio of the typical leaf size to the canopy height. When s_l goes to zero this situation corresponds to a canopy with small leaf size (needle-like) resulting in a bright hot spot. On the other hand, when the hot spot parameter tends to infinity this situation corresponds to a canopy with big leaves (banana-like) or no hot spot. As can be seen from fig. 6 and figure 7 the reflectance ratio RGVI and RRVI are nearly independent on the hot spot parameter for low LAI's. But, for high LAI (LAI = 10) a decrease of the reflectance ratio RRVI of about 15% is observed when the hot spot parameter increases from zero to 2.

For dense vegetation (LAI = 10) the reflectance ratio RRVI shows the same trend in a more pronounced way. The decrease of the reflectance ratio reaches about 24 %.

In order to come to an approximation, it is proposed to assume that both reflectance ratios are independent of the hot spot parameter for all LAI and can be approximated by a mean reflectance ratio valid for each LAI. For a LAI of 10 the average RGVI will be 7.9 ($\pm 6.5\%$) while RRVI will be 19.1 ($\pm 9.4\%$).

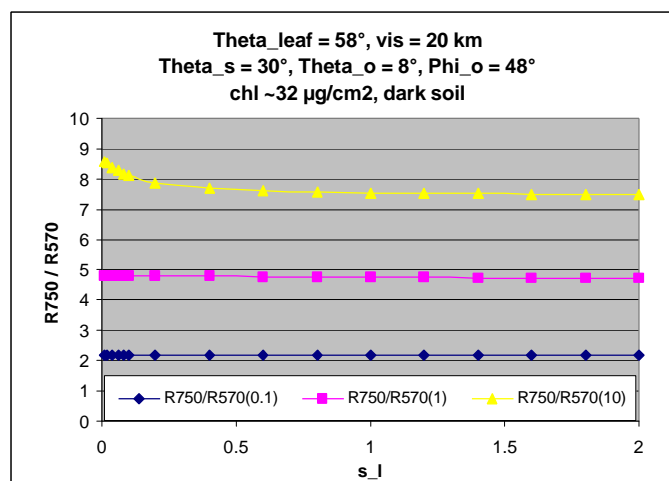


Figure 6: Reflectance ratio RGVI as a function of the hot spot parameter s_l for different leaf area indices (LAI=0.1; LAI=1; LAI=10).

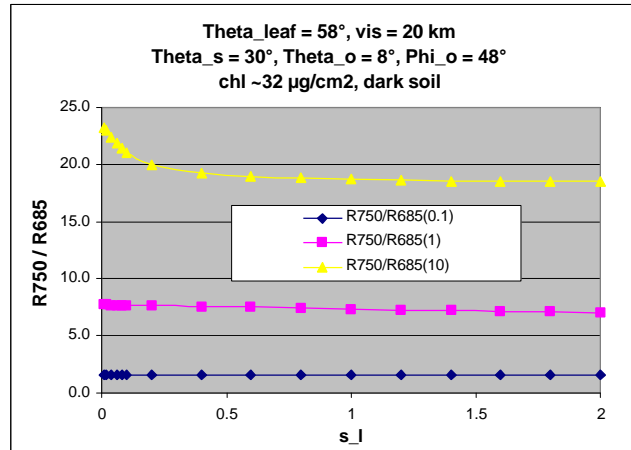


Figure 7: Reflectance ratio RRVI as a function of the hot spot parameter s_l for different leaf area indices (LAI=0.1; LAI=1; LAI=10).

3.1.2.5 Influence of leaf area index (LAI) and leaf angle distribution function (LADF)

In the previous section it could be observed that the new VI's also increase with increasing leaf area index (LAI) as it is known for the AVHRR_NDVI. Systematic investigations were performed for quantifying the dependence of the RRVI and the RGVI with the LAI.

For dark green leaves (chlorophyll content $32 \mu\text{g}/\text{cm}^2$) the increase of reflectance ratio RGVI with LAI depends on the canopy architecture (figure 8). For an erectophile leaf angle distribution (75°) a nearly linear correlation can be found with $r^2 = 0.989$. The linear fit gives an interception of about 1.87 and a slope of about 1.08. For a random and planophile architecture a non-linear increase is observed with a saturation beyond an LAI of 3 – 4. This functional dependence is comparable with the behavior of the AVHRR_NDVI with increasing LAI.

The increase of the RRVI with the LAI also depends on the canopy architecture as shown in figure 9. For an erectophile canopy architecture a linear increase of the RRVI with LAI can be approximated. The correlation coefficient is found to $r^2 = 0.991$. The linear fit gives an interception of about 0.915 and a slope of about 2.259. Compared to the linear increase of RGVI with LAI, a higher dynamic is found for RRVI.

Also, for a random leaf angle distribution a linear increase of the RRVI with LAI can be approximated. The correlation is found to $r^2 = 0.983$ while the interception is 1.26 and the slope is 2.86. For LAI greater than 6, the RRVI becomes saturated and the linear approximation becomes more and more disturbed. Planophile leaf angle distribution results in non-linear increase of the RRVI with LAI as observed for the AVHRR_NDVI. In general, it can be stated that the dynamic of the RRVI in dependence with the LAI is increased compared to the RGVI.

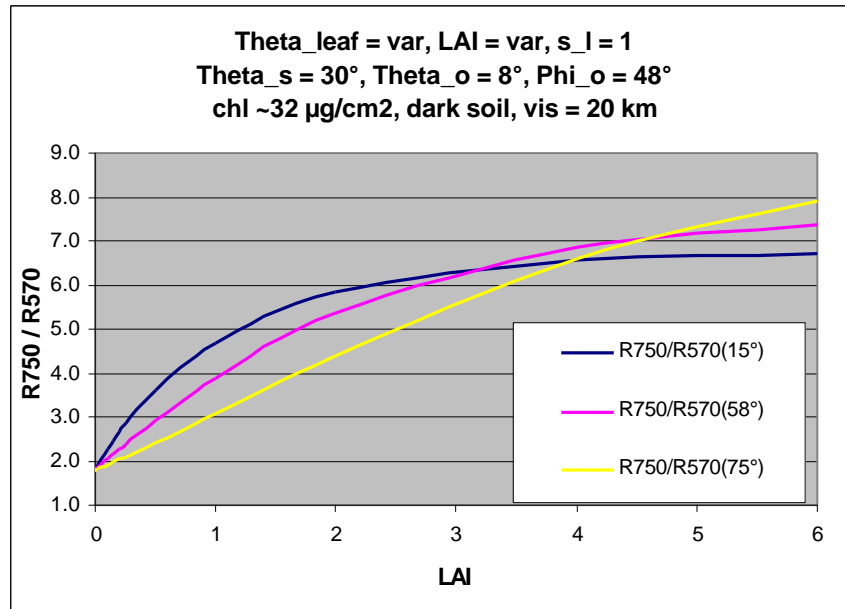


Figure 8: Reflectance ratio RGVI as a function of the leaf area index LAI for different canopy architectures.

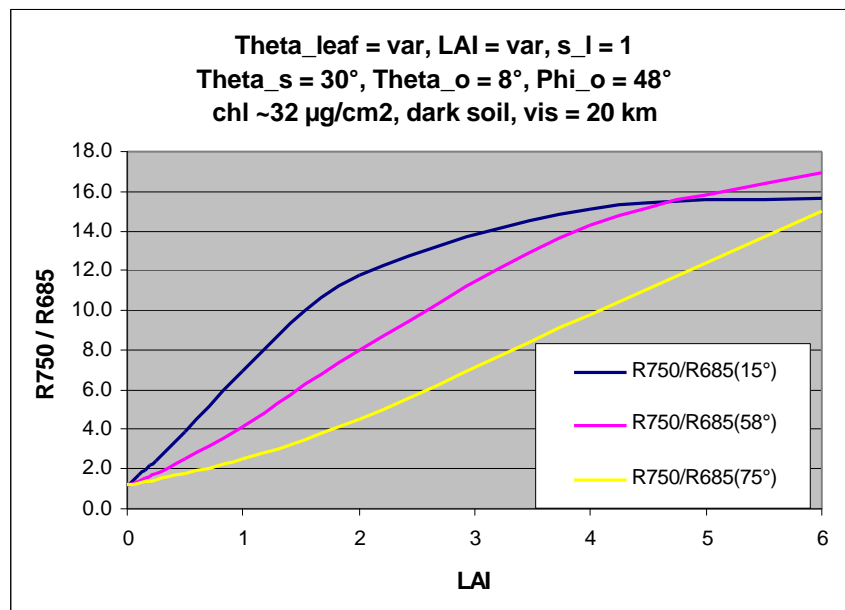


Figure 9: Reflectance ratio RRVI as a function of the leaf area index LAI for different canopy architectures.

3.1.2.6 RRVI depending on leaf chlorophyll content

After analysing the influence of different parameters as e.g. the sun zenith angle, the leaf area index or the hot-spot parameter on the new vegetation index RRVI as defined by Gitelson and Merzylak (1994), the following section summarizes the results of the modeling with respect to the leaf chlorophyll content.

In figure 10, the reflectance ratio RRVI as a function of the leaf chlorophyll content is shown for different LAI and different soil conditions. The suffix "d" means "dark soil" while the suffix "b" means "bright soil". A planophile leaf angle distribution (15°) is assumed.

For a high leaf area index (LAI= 6), the RRVI increases non-linear with the leaf chlorophyll content. Up to a chlorophyll content of about 30 $\mu\text{g}/\text{cm}^2$ a linear correlation is found with a correlation coefficient $r^2 = 0.992$, an interception of 1.32 and a slope of 0.458. Above about 30 $\mu\text{g}/\text{cm}^2$ saturation occurs. No differences between dark and bright soil conditions are observed for high LAI's.

For a LAI of 1, the RRVI also shows non-linear behavior with increasing chlorophyll content but also depending on the soil conditions. For very low LAI, RRVI is independent on the chlorophyll content.

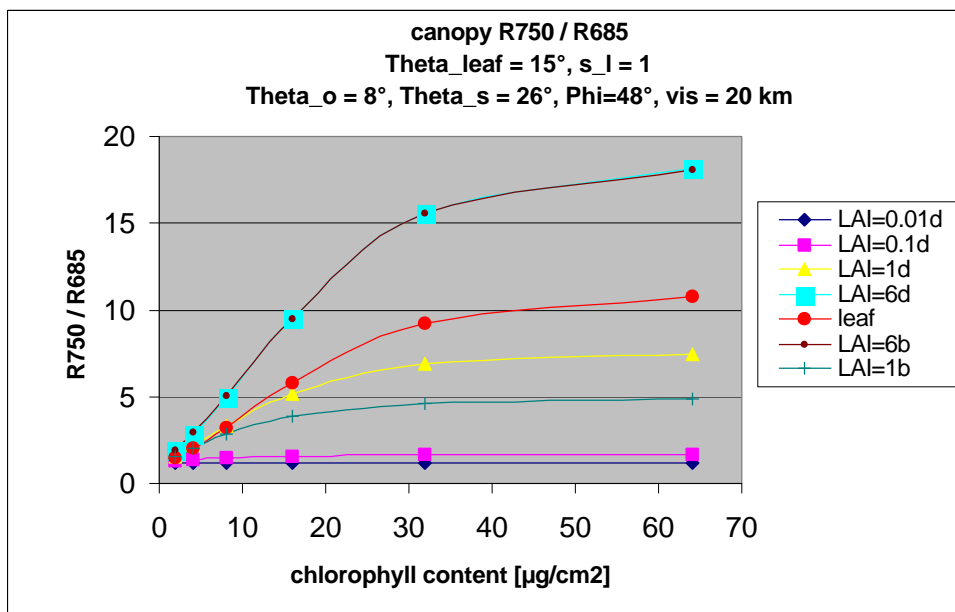


Figure 10: Canopy reflectance ratio RRVI as a function of the leaf chlorophyll content for different LAI and different soil conditions. Planophile canopy architecture. Index d means "dark soil" while index b means "bright soil". For comparison, the RRVI for a single leaf is shown (dotted line in red).

In figure 11 and 12, the functional dependence of the RRVI with the chlorophyll content of leaves is shown for random (figure 11) and erectophile canopy architecture. Again, the leaf area index LAI is chosen as parameter. Even for high LAI, the influence of the soil condition becomes more and more pronounced with increasing leaf angle. For erectophile canopy architecture, a significant difference is observed even for LAI = 6.

For random leaf angle distribution (58°), a good linear correlation can be approximated for LAI = 6 up to about 30 $\mu\text{g}/\text{cm}^2$, with a correlation coefficient $r^2 = 0.99$, an interception of 1.48 and a slope of 0.489 (dark soil). For a bright soil, the correlation coefficient is $r^2 = 0.98$, the interception is 1.67 and the slope is 0.45.

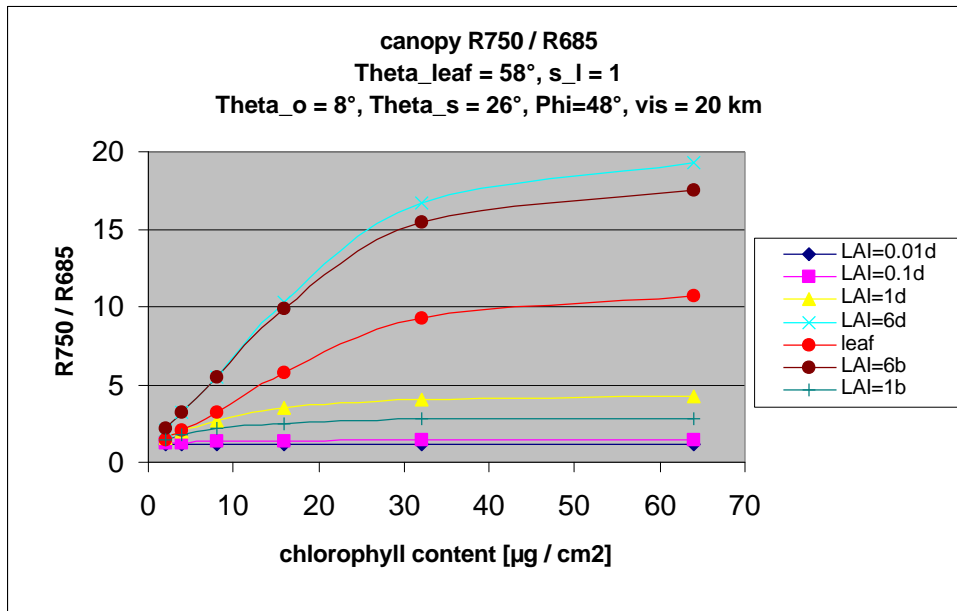


Figure 11: Canopy reflectance ratio RRVI as a function of the leaf chlorophyll content for different LAI and different soil conditions. Random canopy architecture. Index d means "dark soil" while index b means "bright soil". For comparison, the RRVI for a single leaf is shown (dotted line in red).

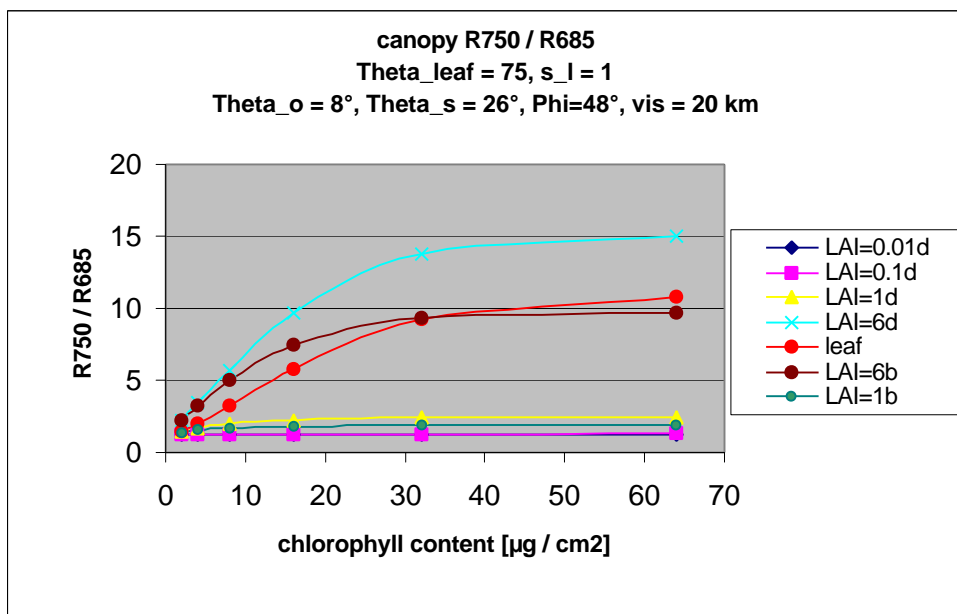


Figure 12: Canopy reflectance ratio RRVI as a function of the leaf chlorophyll content for different LAI and different soil conditions. Erectophile canopy architecture. Index d means "dark soil" while index b means "bright soil". For comparison, the RRVI for a single leaf is shown (dotted line in red).

3.1.2.7 RGVI depending on leaf chlorophyll content

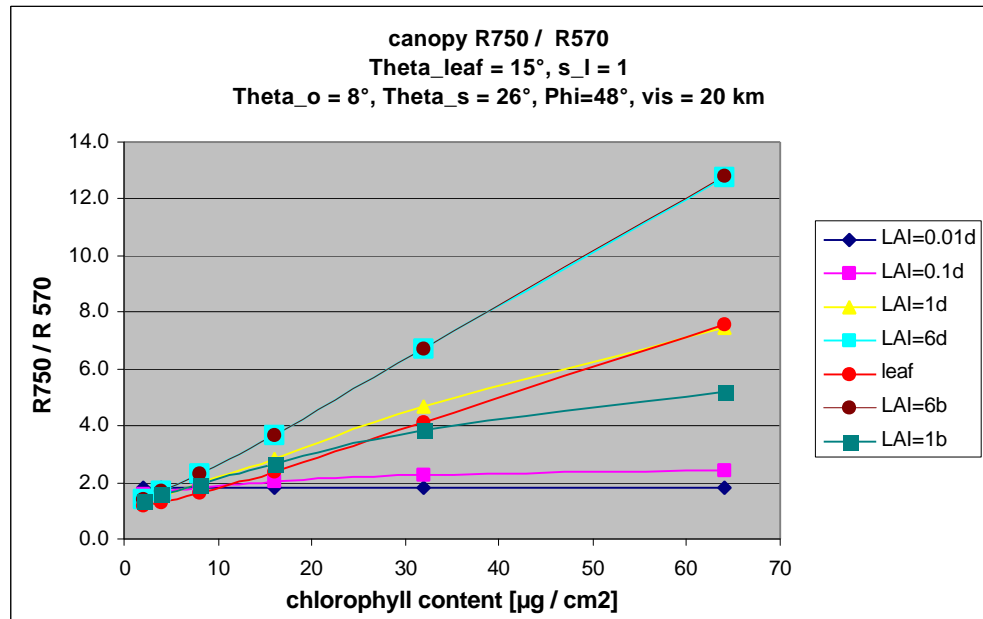


Figure 13: Canopy reflectance ratio RGVI as a function of the leaf chlorophyll content for different LAI and different soil conditions. Planophile canopy architecture. Index d means “dark soil” while index b means “bright soil”. For comparison, the RGVI for a single leaf is shown (dotted line in red).

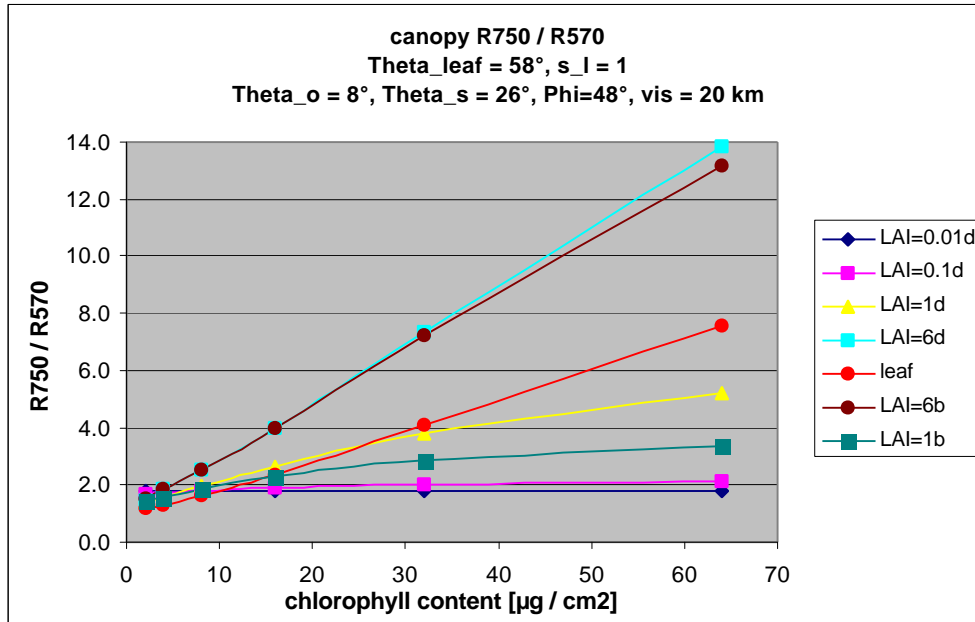


Figure 14: Canopy reflectance ratio RGVI as a function of the leaf chlorophyll content for different LAI and different soil conditions. Random canopy architecture. Index d means “dark soil” while index b means “bright soil”. For comparison, the RGVI for a single leaf is shown (dotted line in red).

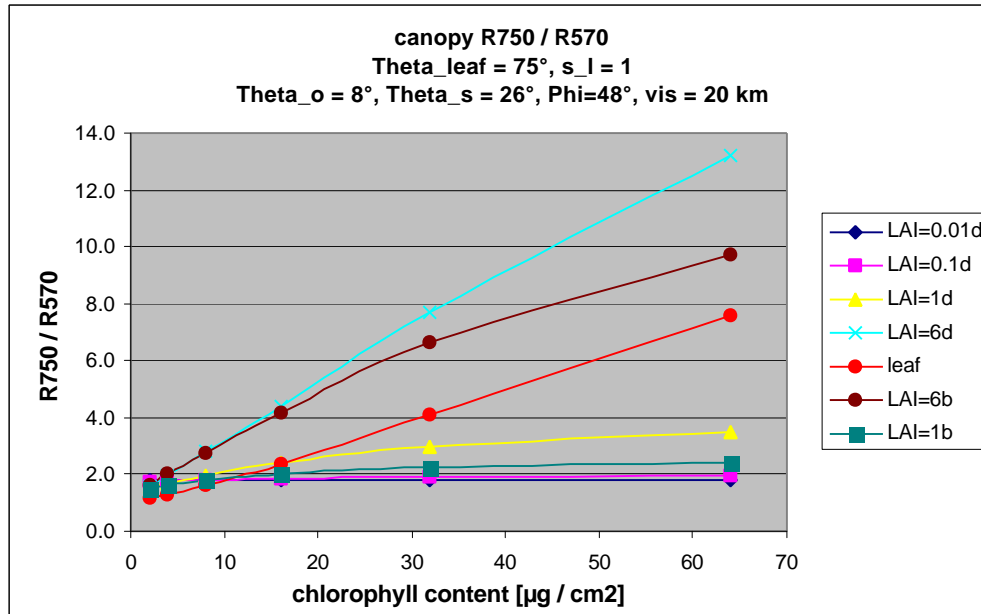


Figure 15: Canopy reflectance ratio RGVI as a function of the leaf chlorophyll content for different LAI and different soil conditions. Erectophile canopy architecture. Index d means "dark soil" while index b means "bright soil". For comparison, the RGVI for a single leaf is shown (dotted line in red).

3.1.2.8 Summary

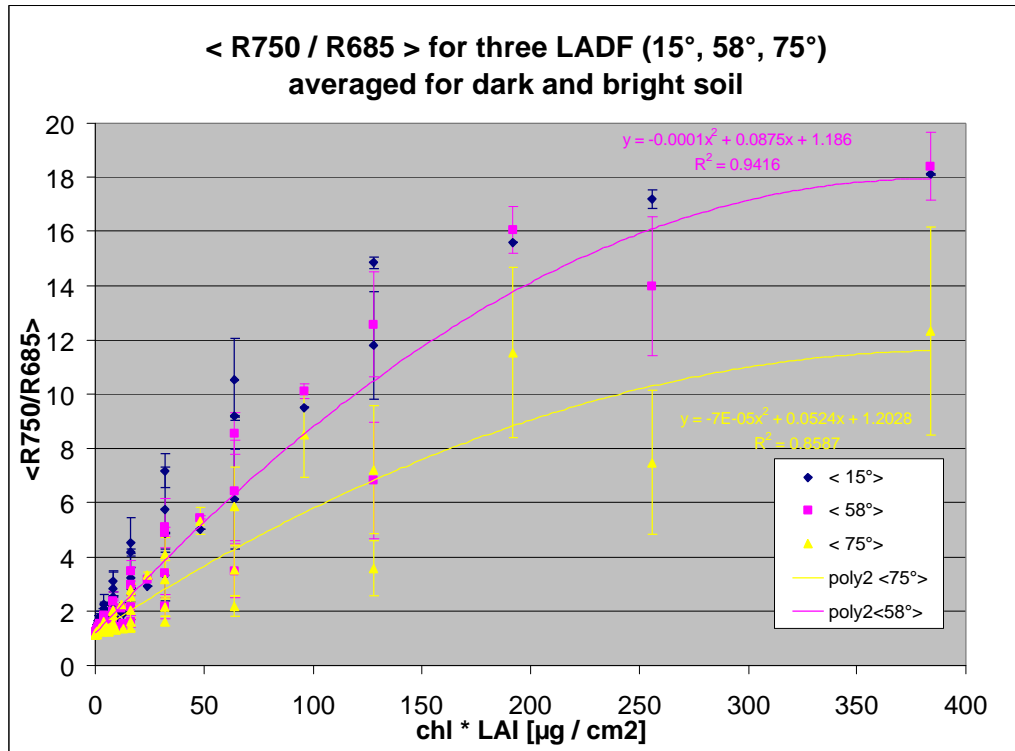


Figure 16: Mean canopy reflectance ratio RRVI as a function of the “canopy chlorophyll content” for three leaf angle distribution functions (planophil, random and erectophil). The reflectance ratio RRVI is averaged over dark and bright soil. Also shown is a polynomial fit of order 2.

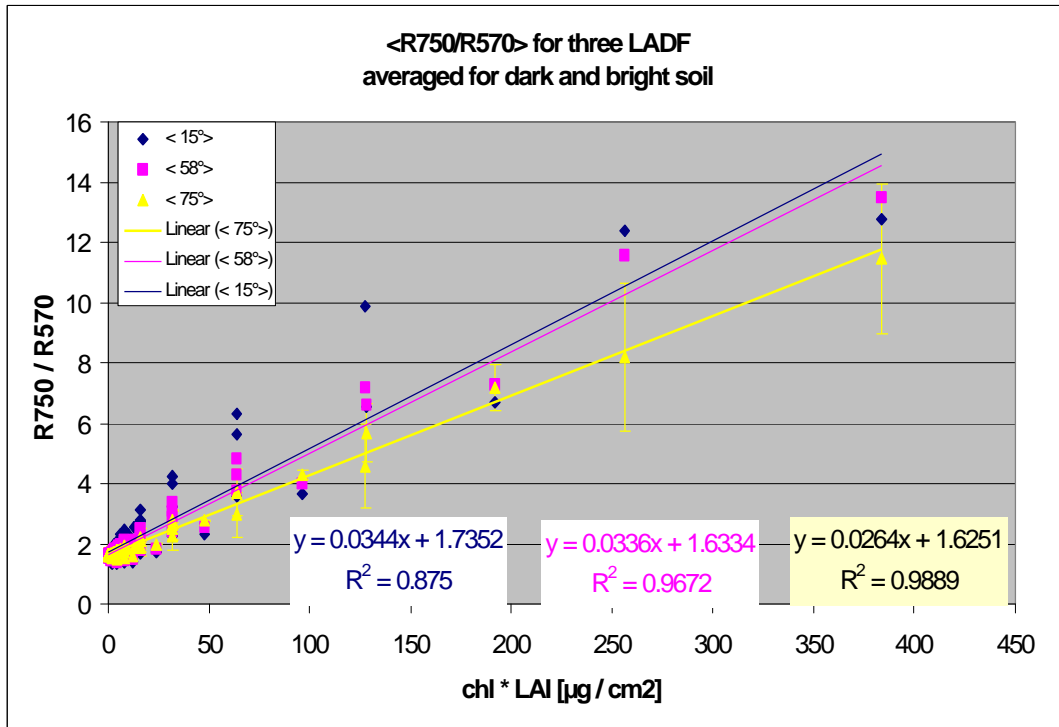


Figure 17: Mean canopy reflectance ratio RGVI as a function of the “canopy chlorophyll content” for three leaf angle distribution functions (planophil, random and erectophil). The reflectance ratio RRVI is averaged over dark and bright soil. Also shown is a linear fit.



MERIS

Doc : MAPP-ATBD-CMAP
Name : Chlorophyll Map
Issue : 1 **Rev** : 0
Date : 08/06/99
Page : 20

3.2 Practical Considerations

For implementation of the algorithm the following flow diagram (fig. 8) is taken as basis



MERIS

Doc : MAPP-ATBD-CMAP
Name : Chlorophyll Map
Issue : 1 **Rev** : 0
Date : 08/06/99
Page : 21

3.2.1 Numerical computation considerations

3.2.2 Calibration and Validation

3.2.3 Exception Handling

Exception handling will be performed according to the flags associated with MERIS level 1 b data as described previous.

3.2.4 Output Products

4. ERROR BUDGET ESTIMATES

5. REFERENCES

Gitelson, A.. A. and Merzlyak, M. N. 1997. Remote estimation of chlorophyll content in higher plant leaves. *Int. J. Remote Sensing*, 18, 2691 – 2697.

Gitelson, A.. A. and Merzlyak, M. N. 1996. Signature analysis of leaf reflectance spectra: Algorithm development for remote sensing of chlorophyll. *J. Plant Physiol.*, 148, 495-500.

Gitelson, A. A., Kaufman, Y. and Merzlyak, M. 1996. Use of a Green Channel in Remote Sensing of Global Vegetation from EOS-MODIS. *Remote Sensing of Environment*, Vol. 58, 289-298.



MERIS

Doc : MAPP-ATBD-CMAP
Name : Chlorophyll Map
Issue : 1 **Rev** : 0
Date : 08/06/99
Page : 22

Gitelson, A. A. and Merzlyak, M. N., 1994. Spectral reflectance changes associated with autumn senescence of *Aesculus hippocastanum* L. and *Acer platanoides* L. leaves. Spectral features and relation to chlorophyll estimation. *J. Plant Physiol.* 143, 286-292.

Jacquemoud, S., Baret, F., Andrieu, B., Danson, F. M. and Jaggard, K., 1995. Extraction of vegetation biophysical parameter by inversion of the PROSPECT + SAIL models on the sugar beet canopy reflectance data. Application to AVIRIS and TM sensors. *Remote Sensing of Environment*, Vol. 52, 163-172.

Lichtenthaler, H.K., Gitelson, A. A. and Lang, M. 1996. Non-destructive determination of chlorophyll content of leaves of a green and an aurea mutant of tobacco by reflectance measurements. *J. Plant Physiol.*, 148, 483-493.

Luedeker, W., and Guenther, K.P. 1990. Leaf reflectance: A stochastic model for analyzing the blue shift, In: *Proc. Symp. on Global and Environmental Monitoring Techniques and Impacts*, Victoria BC (Canada), 17-21 September 1990, 28:475-480.

Maier, S. W., Luedeker, W. and Guenther, K. P. 1999. SLOP: A Revised Version of the Stochastic Model for Leaf Optical Properties, accepted by *Remote Sensing of Environment*.

Major, D.J., Schaalje, G.B., and Wiegand, C. 1992. Accuracy and sensitivity analyses of SAIL model-predicted reflectance of maize, *Remote Sens. Environ.* 41:61-73.

Verhoef, W. 1984. Light scattering by leaf layers with application to canopy reflectance modeling: the SAIL model, *Remote Sens. Environ.* 16:125-141.

6. MAPP DATA PRODUCT SUMMARY SHEET

Product name:	
Product code:	
Product Level:	
Description of the Product:	
Product Parameters:	
Coverage	
Packaging:	



MERIS

Doc : MAPP-ATBD-CMAP

Name : Chlorophyll Map

Issue : 1 **Rev** : 0

Date : 08/06/99

Page : 23

Units:	
Range:	
Sampling:	
Resolution:	
Accuracy:	
Geo-location:	
Format:	
Appended data:	
Frequency of generation:	
Size of product:	
Additional information:	
Identification of bands used in algorithm	
Assumption on MERIS input data	
Identification of ancillary and auxiliary data	
Assumptions on ancillary and auxiliary data	

7. ACKNOWLEDGEMENT

We may thank Stefan Jacquemoud; University of Paris, France, very much, who supported our work by delivering his coupled PROSPECT-SAIL model. Based on this source code, we were able to develop our coupled SLOP-SAIL model in a very condensed form. The version is now running on PC's by calling macro functions in an EXCEL sheet.

We may also thank Mark Danson from the University of Salford, UK, for the development of a SAIL teaching model which is available for public use and was a good introduction to canopy reflectance.